Allometry of hummingbird lifting performance

D. L. Altshuler[1,*], R. Dudley[2,3], S. M. Heredia[4] and J. A. McGuire[2,5]

[1]Department of Biology, 900 University Avenue, University of California, Riverside, CA 92521, USA, [2]Department of Integrative Biology, University of California, Berkeley, CA, 94720 USA, [3]Smithsonian Tropical Research Institute, PO Box 2072, Balboa, Republic of Panama, [4]Department of Botany and Plant Sciences, University of California, Riverside, CA 92521, USA and [5]Museum of Vertebrate Zoology, 3101 Valley Life Sciences Building, University of California, Berkeley, CA, 94720, USA

*Author for correspondence (douga@ucr.edu)

SUMMARY

Vertical lifting performance in 67 hummingbird species was studied across a 4000 m elevational gradient. We used the technique of asymptotic load-lifting to elicit maximum sustained muscle power output during loaded hovering flight. Our analysis incorporated direct measurements of maximum sustained load and simultaneous wingbeat kinematics, together with aerodynamic estimates of mass-specific mechanical power output, all within a robust phylogenetic framework for the Trochilidae. We evaluated key statistical factors relevant to estimating slopes for allometric relationships by performing analyses with and without phylogenetic information, and incorporating species-specific measurement error. We further examined allometric relationships at different elevations because this gradient represents a natural experiment for studying physical challenges to animal flight mechanics. Maximum lifting capacity (i.e. vertical force production) declined with elevation, but was either isometric or negatively allometric with respect to both body and muscle mass, depending on elevational occurrence of the corresponding taxa. Maximum relative muscle power output exhibited a negative allometry with respect to muscle mass, supporting theoretical predictions from muscle mechanics.

Supplementary material available online at http://jeb.biologists.org/cgi/content/full/213/5/725/DC1

Key words: allometry, body size, elevation, flight, load-lifting, maximum performance, muscle power output.

INTRODUCTION

Allometric limits to animal flight performance may derive from either energetic or aerodynamic constraints. In the former case, the relative power output of flight muscle is expected to decrease with increasing body size. In particular, contractile force of muscle is proportional to its cross-sectional area (i.e. to the number of myofibrils), which exhibits a relative decline with increasing muscle volume (i.e. mass). Contractile speed and thus frequency of repetitive contraction also must decrease with increasing muscle length (Hill, 1950). Declines with size in both the relative force and absolute speed of muscular contraction yield a negative allometry in mass-specific mechanical power output such that an increasing body size eventually surpasses an energetically limiting threshold (Pennycuick, 1968; Pennycuick, 1975). In the latter case of aerodynamic limits to flight performance, either physical limits to mechanisms of force production (Ellington, 1991) or anatomical constraints on wing motions (e.g. Chai and Dudley, 1995) limit flight capacity, independently of the total power potentially produced by the muscle. Either power or aerodynamic force production may therefore be limiting according to the particular behavioral and biomechanical context under consideration. The load-lifting performance of flying animals has received particular attention because these theoretical models suggest that the relative ability to lift and sustain weights aloft should decline at increased body mass given an adverse increase in the relative cost of flight.

In a comprehensive study, Marden measured the capacity of 68 species of insects, birds and bats to take off with cumulatively added loads (Marden, 1987). These measurements revealed an isometric relationship between maximum lifted load and the muscle mass of the entire flight motor (i.e. flight muscles in the thoracic and/or pectoral regions as well as those in the wings, when present). This result is not an expectation of either energetic or aerodynamic theory (but see Bejan and Marden, 2006; Ellington, 1991). Nonetheless, this result has since been confirmed for a much broader range of biological motors, including the muscles of swimming fish and running terrestrial animals, as well as human-made motors such as piston engines and jets (Marden, 2005; Marden and Allen, 2002).

The scaling relationships of maximum muscle power output during flight have been analyzed in multiple studies using aerodynamic estimates of power, sometimes in combination with *in vivo* recordings of muscle activation, length changes and force production. However, no consistent relationship between maximum power output and body size has yet emerged. Using aforementioned load-lifting data, Marden (Marden, 1994) estimated that maximum power output per unit muscle mass was positively allometric for flying animals. This conclusion was supported by Chai and Millard (Chai and Millard, 1997) for four species of hummingbirds. By contrast, Tobalske and Dial (Tobalske and Dial, 2000) found that mechanical power output during take-off scaled negatively relative to body size in four species of the avian family Phasianidae. Askew et al. (Askew et al., 2001) studied muscle performance in another member of the pheasant family (the blue-breasted quail *Coturnix chinensis*) and re-analyzed the data from Tobalske and Dial (Tobalske and Dial, 2000), concluding that for Phasianidae as well as some other birds, maximum mechanical power scaled isometrically with respect to body mass.

Determining how physiological performance scales across multiple taxa is challenging for several reasons. First, it is difficult

to attain meaningful and functionally equivalent performance measures for a large number of taxa. Second, muscle physiology and architecture can vary considerably across taxa. Third, the evolutionary relationships among taxa add hierarchical structure to the data that alters expected statistical distributions and accordingly inflates type I error rates when using traditional statistical methods (Felsenstein, 1985). Of the aforementioned studies, only Tobalske and Dial (Tobalske and Dial, 2000) implemented phylogenetic controls required for appropriate statistical analysis of interspecific data. Finally, the most commonly used and available statistical approaches for estimating slopes, including least squares regression and reduced major axis regression, do not incorporate the effects of within-species variation or measurement error. Failure to account for such variation in both performance and body size can lead to imprecise estimates of the slopes (Ives et al., 2007).

Here, we evaluate the allometry of wingbeat kinematics, vertical force production, and associated muscle power output by comparing the maximum load-lifting performance of 67 species of hummingbirds. This data set is analyzed in conjunction with a robust multilocus phylogenetic hypothesis derived for 151 trochilid species (McGuire et al., 2007). The analyses were performed using techniques for analyzing phylogetically correlated data that include within-species variation (Ives et al., 2007).

For comparing allometric relationships, it is useful to identify theoretical expectations under geometrically similar design (i.e. isometry). Although flight performance variables are not geometric quantities, we can estimate isometric expectations referenced to mass-mass relationships, which will scale with a slope of one under geometric similarity. This value characterizes the isometric hypothesis for regressions between maximum lifted mass and either body mass or muscle mass. Mass-specific power output regressed against mass will accordingly have an expected slope of zero under isometry. However, physiological considerations suggest an alternative expectation of negative allometry for mass-specific power output. Muscle power output can be modeled as the product of muscle stress, strain, and contraction frequency (see Ellington, 1991; Hill, 1950). Both maximum myofibrillar stress and maximum muscle strain are expected to be size independent, whereas contraction (i.e. wingbeat) frequency will scale inversely with wing length and thus under isometry as mass$^{-1/3}$. Muscle-mass-specific power output is thus predicted to scale with a similarly negative allometry. Here, we consider the expectation of isometry under the mass-mass relationship as the simplest potential explanation of the data and according apply this expectation as our null.

Hummingbirds occur across a broad range of elevations, and our previous studies have demonstrated a strong influence of both air density and oxygen availability on hovering ability (Altshuler, 2006; Altshuler and Dudley, 2003; Altshuler et al., 2004b; Chai and Dudley, 1995; Chai and Dudley, 1996). Here, we decouple altitudinal from allometric effects by grouping hummingbird taxa into distinct elevational bands for which scaling coefficients of flight performance are calculated separately. We then compare these coefficients among elevational bands to examine how lifting performance changes with altitude.

MATERIALS AND METHODS
Field sites

We studied hummingbird lifting performance at eleven sites in the Peruvian Andes between June 1997 and August 2000 [for specific locations see Altshuler et al. (Altshuler et al., 2004b)], at two sites in the Rocky Mountains of Colorado between June 1998 and August 1999 (for details, see Altshuler and Dudley, 2003), and at five sites in Costa Rica (see Table S1 in supplementary material) between August and September 2003. Site elevations were determined using barometers and regional topographic maps. Associated values for the partial pressure of oxygen, mass density of air, and dynamic viscosity were calculated using formulae from Reid et al. (Reid et al., 1987) and Denny (Denny, 1993). Although diurnal temperature and atmospheric pressure fluctuations characterized all sites and locally influenced air properties among site-specific trials, such effects are typically very small relative to the large changes in air density and oxygen partial pressure across a 4000 m study gradient (see Dudley and Chai, 1996).

Hummingbirds were captured using mist nets, drop-door traps, or Hall traps, and were immediately transported to a field laboratory for morphological measurements and flight trials. Only non-molting individuals were included in the present analyses.

Morphology

Hummingbird body mass was measured to within 0.001 g using an Acculab digital balance (PP-2060D). Wings were photographed against a background of graph paper and were digitized using either NIH Image or ImageJ software to yield chordwise measurements of wing shape that were further analyzed to determine wing length, wing area, aspect ratio and the moments of wing area (Ellington, 1984a). During the six years of this study, 14 hummingbirds died inadvertently during capture, experimental trials, or when otherwise in captivity. Immediately upon death, body mass of these birds was measured and then the pectoralis major and supracoracoideus muscles from both sides were dissected out and weighed. The mass data were combined with published information on hummingbird muscle and body masses from other taxa (Chai and Millard, 1997; Hartman, 1954; Wells, 1993) for correlation analysis between these variables.

Kinematics

Chai et al. (Chai et al., 1997) first described an asymptotic load-lifting assay for ruby-throated hummingbirds, and many authors have subsequently employed this technique to evaluate maximal performance in bees and in other hummingbirds (Altshuler, 2006; Altshuler and Dudley, 2003; Altshuler et al., 2004b; Chai and Millard, 1997; Dillon and Dudley, 2004).

In the first paper of this series we presented a thorough description of the method and we provide only a brief account here. Hummingbirds lifted weights and attained maximum load while hovering within a chamber (0.45 m×0.45 m×0.9 m; length × width × height) constructed from either opaque acrylic or dark nylon mesh walls and a roof made of clear acrylic. At the beginning of a load-lifting trial, we placed a rubber band harness over the head of the hummingbird, which was connected ventrally to a thread containing color-coded beads affixed so as to yield a constant linear mass density along its length. We then released the hummingbird from the floor of the chamber, and the animals exhibited a typical escape response by flying upwards and thus lifting progressively more weights asymptotically to the point of maximum vertical force production in hovering flight. Upon reaching the greatest height (and thus greatest sustained weight), hummingbirds briefly maintained vertical and horizontal position for multiple wingbeats before gradually descending to the walls or floor of the chamber.

We filmed the floor of the chamber at 30 frames s^{-1} using a single camera, either analog (Sony Video 8XR CCD-TRV16) or digital (JVC GR-DV800U), which recorded the number of weight units remaining unlifted and thus, by subtraction, the weight lifted by the hummingbird. We used a second camera, either analog (Sony Video

8 CCD-TR44 operated at 60 fields s^{-1}) or digital (Redlake MotionMeter operated at 500 frames s^{-1}) to record the horizontal projection of wingbeat kinematics as viewed through a large mirror positioned at 45 deg. above the chamber. We synchronized the weighted thread camera and the wingbeat camera using either internal camera clocks or a common trigger, facilitating identification of both views for any particular lifting sequence.

We identified sequences in which birds lifted the greatest weight, but restricted our analyses to those lifting plateaus during which the hummingbirds did not substantially change their horizontal or vertical positions for at least 0.5 s (typically dozens of wingbeats), and were at least two and one-half wing lengths from any surface of the flight chamber. For lifting plateaus that met these criteria, we analyzed up to three separate sequences for any given bird. Following load-lifting trials, we filmed free hovering flight by each hummingbird in the same flight chamber. Wingbeat kinematics were determined from frame-by-frame analysis of the dorsal video perspective. For recordings made with the slower analog video, wingbeat frequency was determined using the interaction frequency between the wingbeat frequency and the filming rate (see Chai and Dudley, 1995; Chai and Dudley, 1996). The much higher temporal resolution of the Redlake digital camera permitted direct frame-by-frame counting to evaluate wingbeat frequency. Stroke amplitude was determined from wing positions at the maximum and minimum positional angles within the nominally horizontal stroke plane. For individuals with multiple analyzed lifting bouts, kinematic parameters for each of the maximum lifts were averaged.

Mechanical power estimates

Power requirements for hovering flight at maximum load were estimated (in units of W kg^{-1}) relative to muscle mass using the aerodynamic equations derived by Ellington (Ellington, 1984b). Specifically, we used the physical properties of air at each site together with the morphological and kinematic data to calculate induced and profile power requirements for maximally loaded flight. Parasite power, which is zero by definition in hovering flight, was ignored. Furthermore, we did not consider here the inertial power requirements for accelerating and decelerating the wings because the degree of elastic energy storage, although probably high, has not been quantified for any hummingbird.

Ellington's (Ellington, 1984b) model requires knowledge of two kinematic parameters that were not available for our data set, the stroke plane angle and the time course of wingtip position. Two previous studies have examined wingtip motion during hummingbird hovering, and concluded that the stroke plane angle was 11 deg. for *Florisuga fusca* (Stolpe and Zimmer, 1939) and 6 deg. for *Archilochus colubris* (Chai et al., 1997). Both values are reasonably close to horizontal plane so we assumed a stroke plane angle of 0 deg. for the hummingbirds in our sample; the energetic estimates of Ellington (Ellington, 1984b) use, in any event, the horizontal projection of the stroke amplitude, which we measured here directly. Also, Weis-Fogh (Weis-Fogh, 1972) analyzed the high-speed kinematic data obtained by Stolpe and Zimmer (Stolpe and Zimmer, 1939) for a hovering hummingbird, and demonstrated a very close correspondence between wingtip angular displacement in the stroke plane and sinusoidal motion. We, accordingly, used values for simple harmonic motion to estimate wing angular velocities and accelerations.

Ellington's (Ellington, 1984b) model also requires an estimate for the profile drag coefficient ($C_{D,pro}$) based on the Reynolds number (Re), which yields values considerably lower than those obtained through direct force measurements on real hummingbird wings in continuous rotation (see Altshuler et al., 2004a). We used for all taxa here a single value (0.139) for $C_{D,pro}$, derived from the wing of a female *Selasphorus rufus* at a Re of 5000 and an angle of attack of 15 deg. (Altshuler et al., 2004a). Variation in $C_{D,pro}$ with Re is small over the range relevant to hummingbird flight (see Usherwood and Ellington, 2002a; Usherwood and Ellington, 2002b).

Statistical analysis

We divided the data into four elevational bands for separate analyses (Fig. 1): lowland (40–500 m), mid-montane (1100–1875 m), highland (2650–3100 m) and alpine (3450–4300 m). Some hummingbird taxa occurred over a range of elevations (e.g. *Colibri coruscans*; 500–3860 m), and data for these species included many individuals measured at different sites. We performed all statistical analysis on mean values by species; data for individuals of the same species in any given elevational band were averaged. However, data for specific individuals measured in different elevational bands were used only in the corresponding band-specific analysis.

The phylogenetic hypothesis that served as the historical framework for the statistical analyses was based on an analysis of two nuclear and two mitochondrial markers for 151 hummingbird and 12 outgroup taxa (McGuire et al., 2007). The original branch lengths from the Bayesian analysis were transformed using non-parametric rate smoothing in the program TreeEdit (Rambaut and Charleston, 2002) to generate a chronogram. The root node age was set arbitrarily to determine relative branch lengths.

Several statistical estimation procedures that include measurement error are available for phylogenetic comparisons. These include estimated generalized least squares (EGLS), maximum likelihood (ML), and restricted maximum likelihood (REML). We analyzed our comparative data on lifting performance and muscle power using the MATLAB program Meregphysig.m (Ives et al., 2007). This package also includes a fourth option for analysis using generalized least squares (GLS), which does not incorporate measurement error, and allows for both phylogenetic and non-phylogenetic tests using each of
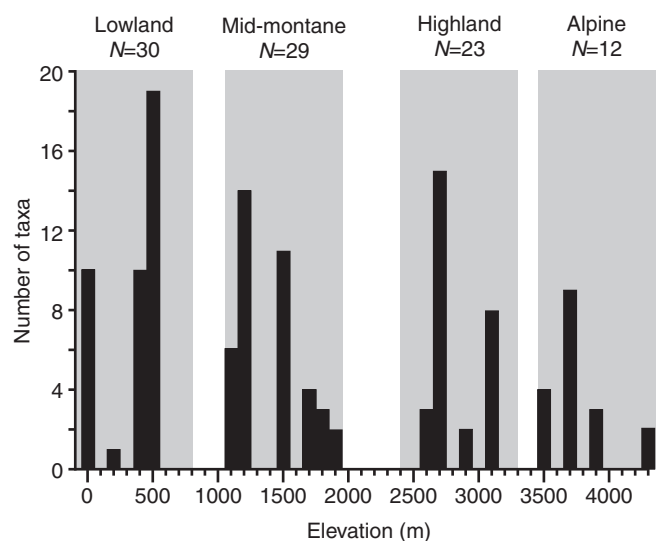

Fig. 1. The number of hummingbird taxa studied at each elevation, including taxa not represented in the phylogeny. Statistical analyses were performed using the elevational bins, indicted by gray bars. The total number of different taxa within each bin is indicated above the bars; sample sizes are lower than the sum of species richness values at each elevation because some taxa were present at multiple sites.

Table 1. Full set of estimates of the intercepts and slopes for the relationships between $\log_{10}$ wingbeat frequency during maximum load-lifting (n_{max}, Hz) and $\log_{10}$ body mass (g) for hummingbird taxa in four elevational bands

Elevation	Phylogeny	Method	Intercept	Slope	Bootstrap estimate	LL
Lowland	I (star)	GLS (no m.e.)	1.8637	−0.4039	−0.4042 (−0.4930, −0.3098)	56.2495
		EGLS	1.8679	−0.4098	−0.4116 (−0.5494, −0.2750)	
		ML	1.8677	−0.4100	−0.4103 (−0.5074, −0.3127)	68.1975
		REML	1.8676	−0.4098	−0.4111 (−0.5098, −0.3119)	
	C (true)	GLS (no m.e.)	1.8764	−0.4057	−0.4063 (−0.5010, −0.3147)	55.8186
		EGLS	1.8834	−0.4148	−0.4148 (−0.5637, −0.2732)	
		ML*	1.8861	−0.4200	−0.4208 (−0.5259, −0.3183)	69.0855
		REML	1.887	−0.4196	−0.4194 (−0.5245, −0.3161)	
Mid–montane	I (star)	GLS (no m.e.)	1.9026	−0.4499	−0.4481 (−0.6169, −0.2803)	32.5154
		EGLS	1.9057	−0.4543	−0.4569 (−0.6633, −0.2656)	
		ML	1.9101	−0.4601	−0.4611 (−0.6460, −0.2947)	41.4311
		REML	1.9096	−0.4597	−0.4579 (−0.6321, −0.2866)	
	C (true)	GLS (no m.e.)	1.8905	−0.4406	−0.4403 (−0.6531, −0.2196)	29.6128
		EGLS	1.8940	−0.4457	−0.4438 (−0.6841, −0.1959)	
		ML*	1.8956	−0.4483	−0.4506 (−0.6941, −0.2216)	43.1771
		REML	1.8955	−0.4477	−0.4435 (−0.6669, −0.2160)	
Highland	I (star)	GLS (no m.e.)	1.9419	−0.5427	−0.5473 (−0.7099, −0.3994)	26.7758
		EGLS	1.9504	−0.5532	−0.5528 (−0.7986, −0.3217)	
		ML	1.9423	−0.5456	−0.5458 (−0.7221, −0.3916)	30.8126
		REML	1.9462	−0.5450	−0.5479 (−0.7216, −0.3760)	
	C (true)	GLS (no m.e.)	1.8800	−0.4628	−0.4661 (−0.6683, −0.2581)	23.5945
		EGLS	1.8971	−0.4821	−0.4821 (−0.7354, −0.2175)	
		ML*	1.8907	−0.4776	−0.4735 (−0.7020, −0.2468)	31.0767
		REML	1.8953	−0.4762	−0.4816 (−0.7069, −0.2558)	
Alpine	I (star)	GLS (no m.e.)	1.8503	−0.4501	−0.4524 (−0.5766, −0.3324)	20.3212
		EGLS	1.8620	−0.4632	−0.4662 (−0.7622, −0.1999)	
		ML	1.8538	−0.4513	−0.4551 (−0.6073, −0.3134)	21.8853
		REML	1.8592	−0.4508	−0.4518 (−0.6049, −0.3052)	
	C (true)	GLS (no m.e.)	1.8282	−0.4238	−0.4232 (−0.5969, −0.2473)	18.7166
		EGLS	1.8384	−0.4338	−0.4380 (−0.7205, −0.1579)	
		ML*	1.8097	−0.4004	−0.4028 (−0.6162, −0.2062)	22.6867
		REML	1.8175	−0.4013	−0.4038 (−0.5926, −0.2180)	

GLS, generalized least squares; EGLS, estimated generalized least squares; ML, maximum likelihood; REML, restricted maximum likelihood.
The models either assumed a star phylogeny (the identity matrix I) or incorporated the true phylogeny (the covariance matrix C). Bootstrapping (N=2000) provided estimates of biases and 95% confidence intervals (mean, lower bound, upper bound). The log likelihoods (LL) were used to select which of the ML models (I *versus* C) best fit the data*.

above approaches. Here, we present results from all eight analytic options, and include bootstrap simulations (N=2000) to estimates slope biases and confidence intervals (Ives et al., 2007).

Which estimation approach and which model are best? These analyses include four classes of models along two axes of consideration. Axis one contains models with and without measurement error. Axis two contains models with and without phylogenetic information. Here, the measurement errors were large enough to affect the parameter estimates so these models are better on first principles. The EGLS, ML and REML estimation procedures are different approaches for analyzing a given measurement-error model. The procedures can be compared in terms of statistical properties, primarily bias and precision, which come from the bootstrap estimates of slope and confidence intervals, respectively. In practice, the REML estimates performed slightly better than the ML estimates in most cases, but in several cases, REML performed distinctly worse. We therefore decided to use ML estimates to compare measurement-error models with and without accounting for phylogenetic relatedness among species. Models with higher likelihoods were considered to be more strongly supported.

Our muscle mass data were much more limited in sample size per species, and it was thus not possible to include measurement error in the statistical models. Instead, we analyzed the relationship between muscle mass and body mass using several regression models including non-phylogenetic ordinary least squares (OLS), phylogenetic generalized least squares (GLS), and phylogenetic regression with an Ornstein-Uhlenbeck (RegOU) process to model evolution of trait residuals. The latter includes an extra parameter and will necessarily have a larger likelihood. We therefore used a log likelihood ratio test to determine if the RegOU was significantly better than other estimates. These analyses were implemented in the MATLAB program Regressionv2.m (Lavin et al., 2008).

RESULTS

We obtained load-lifting and morphological data from 677 individual hummingbirds representing 75 taxa ranging over an altitudinal gradient from sea level to 4300 m. Some taxa were found within more than one elevational band, but specific data for such individuals were only used at the corresponding elevation of capture. Of all study species, 67 taxa were represented in the available phylogeny, and this taxonomic subset was used for
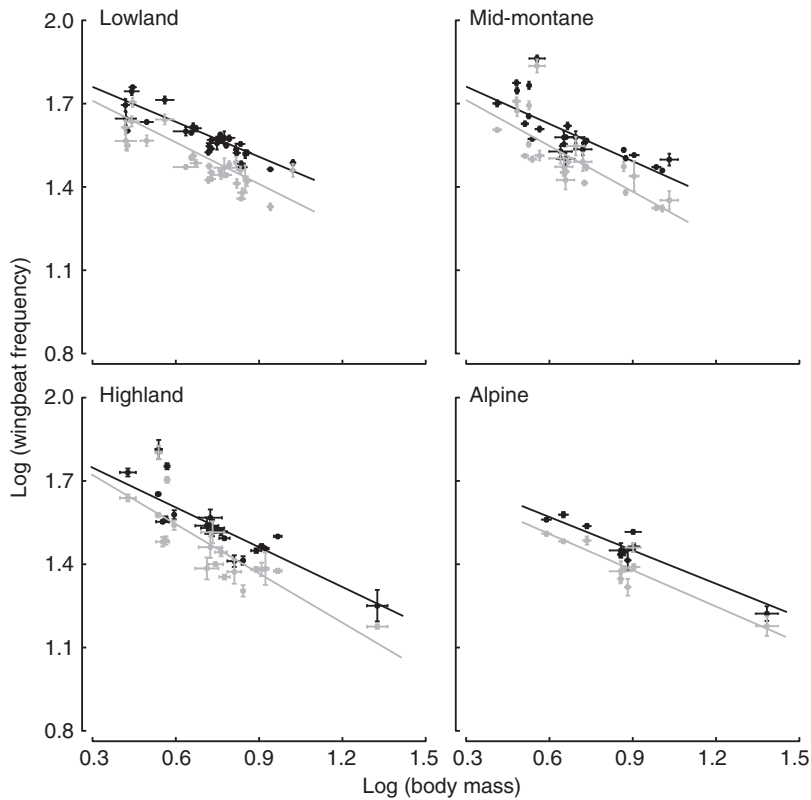
Fig. 2. The relationship between $\log_{10}$ wingbeat frequency and $\log_{10}$ body mass for four elevational bins: lowland, mid-montane, highland and alpine taxa. Circles represent species means and bars represent standard errors along both axes. Values in gray are for normal non-loaded hovering, and values in black for maximum load-lifting. The solid lines provides the best-fit slopes and intercepts, as given in Tables 1 and 2.

kinematics and power analyses using both phylogenetic and non-phylogenetic approaches. The mean values for morphological, kinematic and lifting data for each taxon are provided in supplementary material Table S2).

Kinematics

The results of the complete set of analyses for the relationship between maximum wingbeat frequency during load-lifting and body mass are given in Table 1. Eight analyses were performed for each elevational band, and these allow for comparisons among models and estimation procedures. As stated above, we focus on ML models and compare likelihood values with and without phylogenetic information. For the specific analysis of maximum wingbeat frequency, measurement-error models that included phylogenetic information performed better than those without it. The complete set of analyses for the remaining hovering wingbeat frequency, stroke amplitude, lifting performance and energetics data are provided in supplementary material Tables S3–S6, S9 and S10 in the online supporting information. The most strongly supported ML models (I versus C) are also presented in the main tables that follow.

Maximum wingbeat frequency declined sharply with increased body mass at all elevations, and the associated regression slopes became progressively steeper from lowland to mid-montane and then to highland assemblages. However, this decline with elevation did not extend to alpine hummingbirds. Similar trends were observed for wingbeat frequencies in unloaded hovering (Table 2), but the hovering values were lower at all body mass values relative to values in maximum load-lifting (Fig. 2). Within each elevational band, the slopes of the regression were more steeply negative for hovering flight than for maximum load-lifting, indicating that larger hummingbirds have a greater capacity to modulate this kinematic feature.

As has been previously documented, hummingbirds increased their stroke amplitude during maximum load-lifting as compared to unloaded hovering (Altshuler and Dudley, 2003; Chai et al., 1997; Chai and Millard, 1997) (supplementary material Tables S4 and S5). In the present analysis, the slopes of the relationships between stroke amplitude (in either maximal load-lifting or hovering) and body mass were not significantly different from zero for any of the elevational bands.

Vertical force production

Total lifted mass equals the combined mass of the body and weights that a hummingbird lifted asymptotically, and for all study species averaged 277% (range 177–390%) of body mass. Considering all individuals separately, the mean relative value for total lifted mass was essentially the same (279%) but the range (159–501%) was broader. In the lowlands, total lifted mass demonstrated positive allometry with respect to body mass (Fig. 3, Table 3). The slopes of the log–log relationships declined at higher elevations, and the values for alpine hummingbirds had an

Table 2. The most strongly supported estimates of the intercepts and slopes for the relationships between $\log_{10}$ wingbeat frequency during normal hovering (n_{hov}, Hz) and $\log_{10}$ body mass (g) for hummingbird taxa in four elevational bands

Elevation	Phylogeny	Intercept	Slope	Bootstrap estimate
Lowland	C (true)	1.8598	−0.4996	−0.5002 (−0.6194, −0.3865)
Mid–montane	I (star)	1.8774	−0.5498	−0.5495 (−0.7600, −0.3416)
Highland	I (star)	1.8982	−0.5910	−0.5933 (−0.8130, −0.3790)
Alpine	I (star)	1.7698	−0.4352	−0.4388 (−0.6258, −0.2575)

All results are from maximum likelihood analysis. Other headings and symbols as in Table 1.
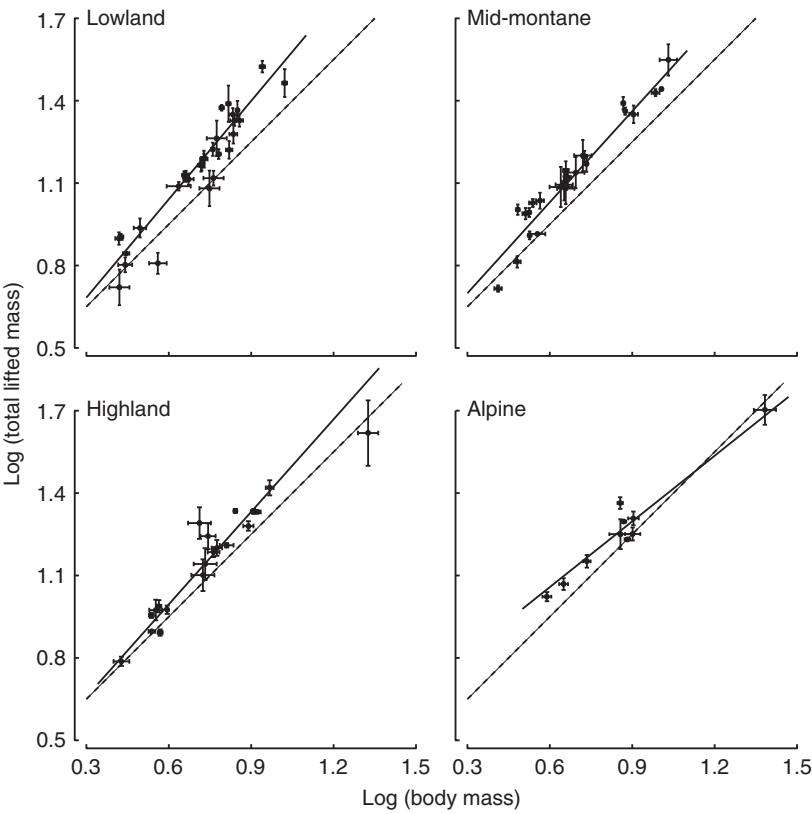
Fig. 3. The relationship between $\log_{10}$ total lifted mass (lifted weights + body mass) and $\log_{10}$ body mass for four elevational bins: lowland, mid-montane, highland and alpine taxa. Circles represent species means, and bars represent standard errors along both axes. The solid line provides the best fit slopes and intercepts, as given in Table 3. The dashed line indicates a slope of 1.

estimated slope of 0.8, which is negatively allometric. However, the 95% confidence intervals for the slopes did not exclude isometry at any elevation.

To express maximum lifting capacity relative to flight muscle mass, we first determined the allometry of muscle mass using data from individual hummingbirds for which relevant morphological variables were available. The body, muscle and heart mass data for the 14 individuals that died over the course of our study are provided in supplementary material Table S7. The data from these 11 species were analyzed in combination with published body and muscle mass data for 13 other species. Of the 24 hummingbird species for which these data were available, 20 species were represented in the phylogeny. We first analyzed the relationships between muscle mass and body mass for these 20 species by comparing non-phylogenetic ordinary least squares (OLS) regression to two models that incorporate phylogenetic association: generalized least squares (GLS) regression and regression with an Ornstein-Uhlenbeck (RegOU) process to model evolution of trait residuals (supplementary

material Table S8). The most strongly supported model was OLS, which was then used for the full data set of 24 species to determine the scaling relationships between muscle mass and body mass (Fig. 4). Muscle mass in hummingbirds exhibits positive allometry. The OLS regression coefficients for the full mass data set were used to estimate muscle masses for additional hummingbird taxa.

At low elevations, the slope of the relationship between total lifted mass and muscle mass was 0.86, but the 95% confidence intervals did not exclude a slope of 1 (Table 4). At higher elevations, the 95% confidence intervals did exclude a slope of 1, indicating that maximum vertical force was negatively allometric with respect to muscle mass (Fig. 5).

Allometry of maximum power output

Muscle-mass-specific aerodynamic power produced during maximum load-lifting scaled negatively with respect to muscle mass at all elevations (Fig. 6, Table 5), with slopes of the log–log regressions becoming progressively more negative at higher elevations.

DISCUSSION

Hummingbirds exemplify both mechanical specializations for enhanced aerodynamic performance, as well as a metabolic extreme of vertebrate design (Altshuler and Dudley, 2002; Suarez, 1992; Suarez, 1996). Biomechanical and physiological adaptations in this taxon are linked to the behavior of sustained nectar feeding from flowers. Study of the limits to hovering ability in hummingbirds can accordingly help to identify general constraints on animal locomotor performance given the high relative expenditure of mechanical and metabolic power associated

Table 3. The most strongly supported estimates of the intercepts and slopes for the relationships between $\log_{10}$ total lifted mass and $\log_{10}$ body mass (g) for hummingbird taxa in four elevational bands

Elevation	Phylogeny	Intercept	Slope	Bootstrap estimate
Lowland	C (true)	0.3249	1.1935	1.1987 (1.0061, 1.4010)
Mid-montane	C (true)	0.3675	1.1045	1.1048 (0.8811, 1.3384)
Highland	I (star)	0.3216	1.1226	1.1278 (0.9494, 1.3071)
Alpine	C (true)	0.5798	0.7966	0.8057 (0.5192, 1.0891)

Total lifted mass = lifted weights + body mass (g).
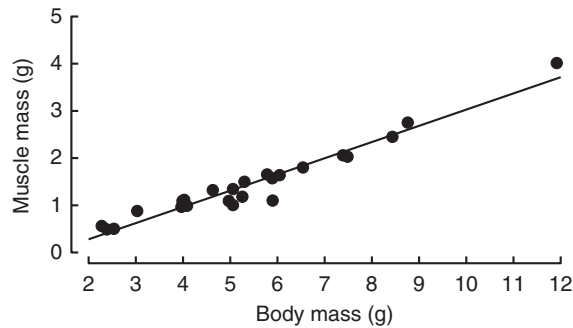All results are from maximum likelihood analysis. Other headings and symbols as in Table 1.

Fig. 4. The relationship between muscle mass and body mass for 24 hummingbird species. Morphological values were not divided into elevational bins. Circles represent species means from the hummingbirds listed in supplementary material Table S7, and also data from other authors as cited in the text. The slope (0.344) and intercept (–0.408) were calculated using ordinary least squares regression, which does not include phylogenetic correction.

with such efforts. We have shown here that maximum lifting capacity scales as positive allometry with respect to body mass at low elevation, but with increasingly declining allometric slopes at higher elevations. However, the 95% confidence intervals for these slopes at all elevations include the value of one. We also examined the scaling of maximum force production with respect to muscle mass, which scales at low elevations with an exponent of 0.86, and declines further with increased elevation. The 95% confidence interval for the slope at lowland elevations again included isometry, but the bounding intervals for slopes at higher elevations did not. The relative capacity of hummingbird flight muscle to produce power exhibits negative allometry at all elevations, with more strongly negative slopes at higher elevations. The strength of these conclusions derives from comparative performance data for more than sixty trochilid species and statistical analysis with controls for both phylogenetic effects and within-species variation.

Scaling relationships of muscle force and power

Maximum vertical force production in flying animals has now been the subject of multiple studies involving diverse taxa, different methodologies, and, in some cases, phylogenetic controls. In each case, the relationship is either at or near to isometry with respect to both body mass and muscle mass (Dillon and Dudley, 2004; Marden, 1987; Marden, 1990; Marden, 1994; Marden, 2005; Marden and Allen, 2002). For hummingbirds, this result may seem particularly surprising given the positive allometry of muscle mass. However, these relationships are best understood by comparing the slopes for the two different variables: the slopes for muscle mass–maximum force relationships are slightly less than one (Table 4), and the slopes for body mass–maximum force relationships are slightly greater than one (Table 3). We have also considered scaling relationships at different elevations and conclude that body-mass-specific maximum force is invariant at all elevations, but that muscle-mass-

specific maximum whole-body forces exhibit negative allometry at mid-montane and higher elevations. An isometric relationship between maximum whole-body force production and either body or muscle mass is predicted by neither aerodynamic nor muscle mechanical theory. Unfortunately, the deviation from isometry in muscle-mass-specific force exhibited by higher elevation taxa does not help to distinguish between either biomechanical or aerodynamic constraints, because both metabolic rate and flight performance may be constrained at higher elevations by lower oxygen availability and by air density, respectively.

If maximum muscle stress and strain scale isometrically, then mass-specific muscle power output should decline linearly with contraction rate and thus with wingbeat frequency of flying animals (Ellington, 1991; Pennycuick, 1975). For hummingbirds, we would thus expect a decline in relative power output at greater body mass given the known negative scaling of the latter quantity (Altshuler and Dudley, 2003; Greenewalt, 1975) (Tables 1 and 2). The present analysis revealed an allometric decline in wingbeat frequency during maximum load lifting in proportion to body mass to the –0.42 (Table 2), a value that is even more negative than the lower confidence limit for the allometry of muscle power output (see Table 5). Major changes in maximum myofibrillar stress are unlikely (Alexander, 1985; Ellington, 1991), and muscle strain must be limited ultimately by the constrained geometry of wing motions that is size invariant among hummingbirds (Altshuler et al., 2004b). Relatively less aerodynamic power must then be available to larger taxa for accelerations and vertical ascent, two behaviors that feature prominently in hummingbird flight biology (Altshuler, 2006).

Our conclusion that maximum flight power is negatively allometric for hummingbirds is congruent with the previously published and phylogenetically controlled study of galliform birds by Tobalske and Dial (Tobalske and Dial, 2000), but not with the expansion and reanalysis of these data presented by Askew et al. (Askew et al., 2001). It also stands in contrast to studies reporting an increase in relative muscle power output with increasing muscle mass (Chai and Millard, 1997; Marden, 1987; Marden, 1994). Our

Table 4. The most strongly supported estimates of the intercepts and slopes for the relationships between $\log_{10}$ total lifted mass and $\log_{10}$ muscle mass (g) for hummingbird taxa in four elevational bands

Elevation	Phylogeny	Intercept	Slope	Bootstrap estimate
Lowland	C (true)	1.0772	0.8558	0.8585 (0.7145, 1.0097)
Mid-montane	C (true)	1.0645	0.8218	0.8232 (0.6662, 0.9905)
Highland	I (star)	1.0200	0.8540	0.8556 (0.7240, 0.9877)
Alpine	C (true)	1.0656	0.6474	0.6490 (0.3992, 0.9056)

Total lifted mass = lifted weights + body mass (in g).
All results are from maximum likelihood analysis. Other headings and symbols as in Table 1.

Table 5. The most strongly supported estimates of the intercepts and slopes for the relationships between $\log_{10}$ maximum aerodynamic power and $\log_{10}$ muscle mass (g) for hummingbird taxa in four elevational bands

Elevation	Phylogeny	Intercept	Slope	Bootstrap estimate
Lowland	C (true)	2.7955	–0.1610	–0.1616 (–0.2964, –0.0317)
Mid–montane	C (true)	2.7939	–0.1727	–0.1746 (–0.3100, –0.0442)
Highland	C (true)	2.7829	–0.2080	–0.2092 (–0.3292, –0.0848)
Alpine	C (true)	2.7932	–0.2536	–0.2789 (–0.6891, 0.0942)

Maximum mass-specific aerodynamic power, $P_{PER}=P_{IND}+P_{PRO}$ (in $W\,kg^{-1}$ muscle).
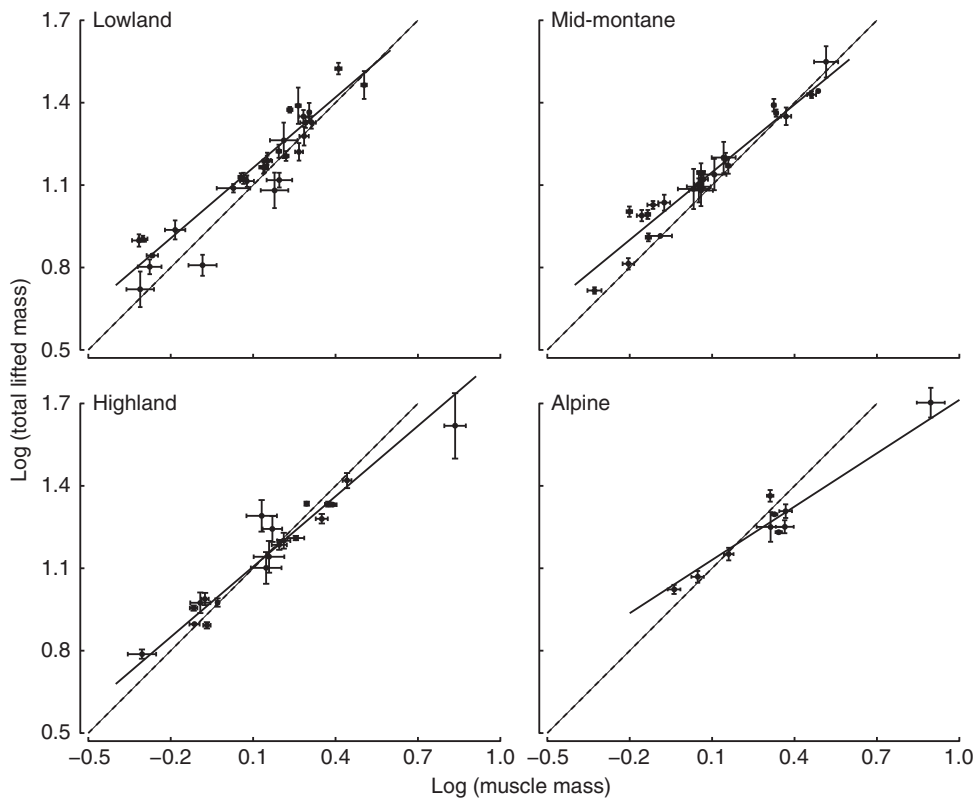Headings and symbols as in Table 1.

Fig. 5. The relationship between $\log_{10}$ total lifted mass and $\log_{10}$ muscle mass for four elevational bins: lowland, mid-montane, highland and alpine taxa. Circles represent species means, and bars represent standard errors along both axes. The solid line provides the best fit slopes and intercepts, as given in Table 4. The dashed line indicates a slope of 1. Muscle mass was estimated from the OLS regression coefficients in supplementary material Table S8.

study is restricted to a monophyletic group that ranges in body mass only by a factor of ten or so, but the finding of significantly negative power allometries is all the more striking given the reduced size range under consideration. Marden (Marden, 1987; Marden, 1990) considered an approximately four orders-of-magnitude range in body sizes of birds, bats and insects, but did not have access to a phylogenetic hypothesis for this diverse group. Another potentially important difference among the studies is that Marden (Marden, 1987) used the full set of flight muscles, including those in the wing, to calculate effective muscle mass, whereas other studies with birds

have used the mass of the pectoral muscles only. It is not known how the wing muscle mass scale relative to the pectoral muscle masses. The demonstration of a relative mass-dependent decline in power output follows predictions of classical muscle mechanics (Hill, 1950), which suggests that phylogenetic approaches may more generally reveal allometries in flight performance that have been otherwise difficult to identify. However, we cannot rule out the alternative hypothesis that lineages of flying animals (e.g. hummingbirds and pheasants relative to other volant taxa) differ in their scaling relationships.
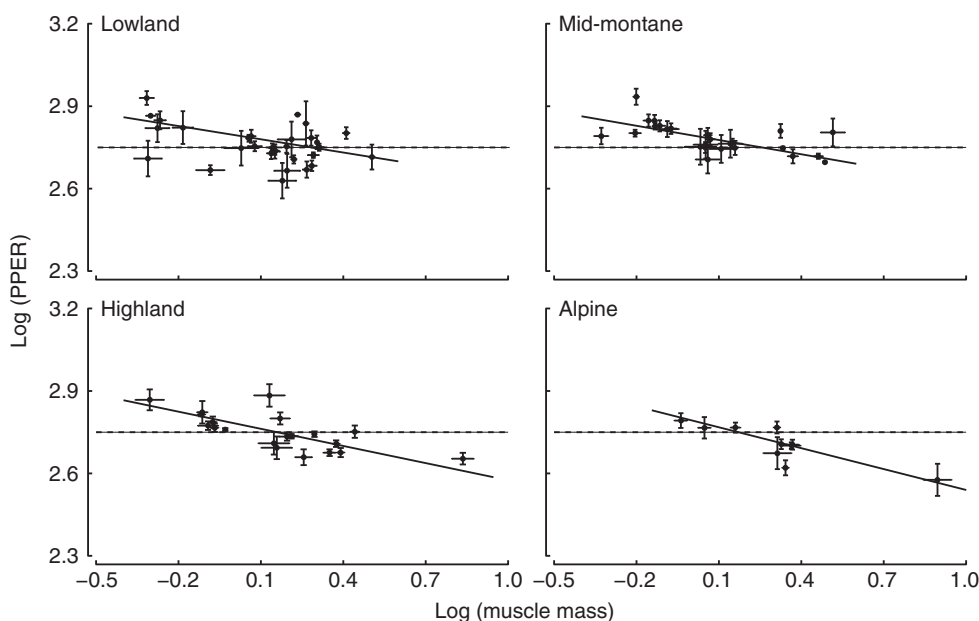

Fig. 6. The relationship between $\log_{10}$ maximum mass-specific aerodynamic power produced during load-lifting and $\log_{10}$ muscle mass for four elevational bins: lowland, mid-montane, highland and alpine taxa. Circles represent species means and bars represent standard errors along both axes. The solid line provides the best-fit slopes and intercepts, given in Table 5. The dashed line indicates a slope of 1. Aerodynamic power was estimated assuming perfect elastic energy storage and based on equations from Ellington (Ellington, 1984b).

Scaling relationships across elevations

Effects of elevational gradients on animal flight performance can be profound and derive from reductions in both air density and oxygen availability (Altshuler and Dudley, 2006; Dillon et al., 2006; Dudley and Chai, 1996). Allometries for both lifting capacity and power production in hovering hummingbirds are also influenced altitudinally such that log–log regression slopes for both variables decline progressively at higher elevations (Figs 3, 5, 6). This adverse outcome may further limit flight abilities in high-altitude birds, and thus supplements our previous finding that power margins for hummingbirds are progressively reduced at higher elevations (Altshuler et al., 2004b). This reduction is mediated mechanistically through systematic increases in stroke amplitude with elevation, combined with an upper angular limit to wing motions within the stroke plane (Chai and Dudley, 1995). Historically, hummingbirds originated in the Neotropical lowlands and subsequently diversified in the mid-montane elevations of the Andes (Bleiweiss, 1998; McGuire et al., 2007). Although associated morphological adaptations [e.g. increased wing length (Altshuler et al., 2004b)] and greater stroke amplitudes in hovering are now known, similar physiological studies of hovering metabolic rates and oxygen-carrying capacity across elevational gradients would complement these aerodynamic studies of flight performance. Oxygen availability has been shown to transcend hypodense aerodynamic limitations for a hovering lowland hummingbird (Chai and Dudley, 1996), but comparable responses in high-elevation trochilids have not yet been studied.

Both high elevation and increased body mass impinge negatively on relative power production by hummingbirds, as mediated by increases in stroke amplitude and reductions in wingbeat frequency, respectively. Pectoral muscle mass exhibits positive allometry among hummingbird species (Fig. 4) (see also Altshuler and Dudley, 2002), possibly in response to the disproportionate dependence of induced power expenditure on body mass raised to the power 1.5 (see Dudley, 2000; Ellington, 1984b). The effects of reduced air density are, however, less pronounced at constant body mass (induced power varies in inverse proportion only to the square root of density), and furthermore will act to reduce expenditure of profile power. Large hummingbirds hovering at high altitude must experience both these effects simultaneously, but have never been studied. In this regard, the giant Andean hummingbird (*Patagona gigas*) would be an experimental subject of great interest given its extreme body mass within the lineage (~22 g) coupled with residence above 4000 m in some populations.

The scaling patterns of hummingbird flight performance relative to body and muscle mass potentially provide insight into the mechanistic bases of such flight behaviors as foraging, agonistic competition, and courtship displays (Feinsinger and Chaplin, 1975; Feinsinger and Colwell, 1978). For example, if maximum force and muscle power scaled isometrically and were invariant across elevations, then success in competitive behaviors related to flight ability might be determined exclusively by body size. However, it is now known that neither foraging behavior nor competitive ability are determined exclusively by flight-related morphological features (Altshuler et al., 2004c), and that the ability to compete successfully can dramatically switch across elevations (Altshuler, 2006). It is now clear that increases in both body size and elevation negatively influence hummingbird flight performance, but overall aerial success must derive from complex interactions among motivational factors, compensatory behaviors, physiological capacity, and the relative flight abilities of competitors.

REFERENCES

Alexander, R. M. (1985). The maximum forces exerted by animals. *J. Exp. Biol.* **115**, 231-238.

Altshuler, D. L. (2006). Flight performance and competitive displacement of hummingbirds across elevational gradients. *Am. Nat.* **167**, 216-229.

Altshuler, D. L. and Dudley, R. (2002). The ecological and evolutionary interface of hummingbird flight physiology. *J. Exp. Biol.* **205**, 2325-2336.

Altshuler, D. L. and Dudley, R. (2003). Kinematics of hovering hummingbird flight along simulated and natural elevational gradients. *J. Exp. Biol.* **206**, 3139-3147.

Altshuler, D. L. and Dudley, R. (2006). The physiology and biomechanics of avian flight at high altitude. *Integr. Comp. Biol.* **46**, 62-71.

Altshuler, D. L., Dudley, R. and Ellington, C. P. (2004a). Aerodynamic forces of revolving hummingbird wings and wing models. *J. Zool.* **264**, 327-332.

Altshuler, D. L., Dudley, R. and McGuire, J. A. (2004b). Resolution of a paradox: Hummingbird flight at high elevation does not come without a cost. *Proc. Natl. Acad. Sci. USA* **101**, 17731-17736.

Altshuler, D. L., Stiles, F. G. and Dudley, R. (2004c). Of hummingbirds and helicopters: Hovering costs, competitive ability, and foraging strategies. *Am. Nat.* **163**, 16-25.

Askew, G. N., Marsh, R. L. and Ellington, C. P. (2001). The mechanical power output of the flight muscles of blue-breasted quail (*Coturnix chinensis*) during take-off. *J. Exp. Biol.* **204**, 3601-3619.

Bejan, A. and Marden, J. H. (2006). Unifying constructal theory for scale effects in running, swimming and flying. *J. Exp. Biol.* **209**, 238-248.

Bleiweiss, R. (1998). Origin of hummingbird faunas. *Biol. J. Linn. Soc.* **65**, 77-97.

Chai, P. and Dudley, R. (1995). Limits to vertebrate locomotor energetics suggested by hummingbirds hovering in Heliox. *Nature* **377**, 722-725.

Chai, P. and Dudley, R. (1996). Limits to flight energetics of hummingbirds hovering in hypodense and hypoxic gas mixtures. *J. Exp. Biol.* **199**, 2285-2295.

Chai, P. and Millard, D. (1997). Flight and size constraints: hovering performance of large hummingbirds under maximal loading. *J. Exp. Biol.* **200**, 2757-2763.

Chai, P., Chen, J. S. C. and Dudley, R. (1997). Transient hovering performance of hummingbirds under conditions of maximal loading. *J. Exp. Biol.* **200**, 921-929.

Denny, M. W. (1993). *Air and Water: The Biology and Physics of Life's Media*. Princeton: Princeton University Press.

Dillon, M. E. and Dudley, R. (2004). Allometry of maximum vertical force production during hovering flight of neotropical orchid bees (Apidae: Euglossini). *J. Exp. Biol.* **207**, 417-425.

Dillon, M. E., Frazier, M. R. and Dudley, R. (2006). Into thin air: Physiology and evolution of alpine insects. *Integr. Comp. Biol.* **46**, 49-61.

Dudley, R. (2000). *The Biomechanics of Insect Flight: Form, Function, Evolution*. Princeton: Princeton University Press.

Dudley, R. and Chai, P. (1996). Animal flight mechanics in physically variable gas mixtures. *J. Exp. Biol.* **199**, 1881-1885.

Ellington, C. P. (1984a). The aerodynamics of hovering insect flight. II. Morphological parameters. *Philos. Trans. R. Soc. Lond. B* **305**, 17-40.

Ellington, C. P. (1984b). The aerodynamics of hovering insect flight. VI. Lift and power requirements. *Philos. Trans. R. Soc. London B* **305**, 145-181.

Ellington, C. P. (1991). Limitations on animal flight performance. *J. Exp. Biol.* **160**, 71-91.

Feinsinger, P. and Chaplin, S. B. (1975). On the relationship between wing disc loading and foraging strategy in hummingbirds. *Am. Nat.* **109**, 217-224.

Feinsinger, P. and Colwell, R. K. (1978). Community organization among neotropical nectar-feeding birds. *Am. Zool.* **18**, 779-795.

Felsenstein, J. (1985). Phylogenies and the comparative method. *Am. Nat.* **125**, 1-15.

Greenewalt, C. H. (1975). The flight of birds. *Trans. Am. Philos. Soc.* **65**, 1-67.

Hartman, F. A. (1954). Cardiac and pectoral muscles of trochilids. *The Auk* **71**, 467-469.

Hill, A. V. (1950). The dimensions of animals and their muscular dynamics. *Science progress* **38**, 209-230.

Ives, A. R., Midford, P. E. and Garland, T. (2007). Within-species variation and measurement error in phylogenetic comparative methods. *Syst. Biol.* **56**, 252-270.

Lavin, S. R., Karasov, W. H., Ives, A. R., Middleton, K. M. and Garland, T. (2008). Morphometrics of the avian small intestine compared with that of nonflying mammals: A phylogenetic approach. *Physiol. Biochem. Zool.* **81**, 526-550.

Marden, J. H. (1987). Maximum lift production during takeoff in flying animals. *J. Exp. Biol.* **130**, 235-258.

Marden, J. H. (1990). Maximum load-lifting and induced power output of Harris' Hawks are general functions of flight muscle mass. *J. Exp. Biol.* **149**, 511-514.

Marden, J. H. (1994). From damselflies to pterosaurs: how burst and sustainable flight performance scale with size. *Am. J. Physiol.* **266**, R1077-R1084.

Marden, J. H. (2005). Scaling of maximum net force output by motors used for locomotion. *J. Exp. Biol.* **208**, 1653-1664.

Marden, J. H. and Allen, L. R. (2002). Molecules, muscles, and machines: Universal performance characteristics of motors. *Proc. Natl. Acad. Sci. USA* **99**, 4161-4166.

McGuire, J. A., Witt, C. C., Altshuler, D. L. and Remsen, J. V. (2007). Phylogenetic systematics of hummingbirds: Bayesian and maximum likelihood analyses of partitioned data and selection of an appropriate partitioning strategy. *Syst. Biol.* **56**, 837-856.

Pennycuick, C. J. (1968). Power requirements for horizontal flight in the pigeon, *Columba livia. J. Exp. Biol.* **49**, 527-555.

Pennycuick, C. J. (1975). Mechanics of flight. In *Avian Biology*, vol. 5 (ed. D. S. Farner and J. R. King), pp. 1-75. London: Academic Press.

Rambaut, A. and Charleston, M. (2002). TreeEdit: Phylogenetic Tree Editor v1.0 alpha 10. http://evolve.zoo.ox.ac.uk/software/TreeEdit/main.html.

Reid, R. C., Prausnitz, J. M. and Poling, B. E. (1987). *The Properties of Gases and Liquids* (4th edn). New York: McGraw-Hill.

Stolpe, V. M. and Zimmer, K. (1939). Der schwirrflug des kolibri im zeitlupenfilm. *Journal fur Ornithologie* **87**, 136-155.

Suarez, R. K. (1992). Hummingbird flight: sustaining the highest mass-specific metabolic rates among vertebrates. *Experientia* **48**, 565-570.

Suarez, R. K. (1996). Upper limits to mass-specific metabolic rates. *Ann. Rev. Physiol.* **58**, 583-605.

Tobalske, B. W. and Dial, K. P. (2000). Effects of body size on take-off flight performance in the Phasianidae (Aves). *J. Exp. Biol.* **203**, 3319-3332.

Usherwood, J. R. and Ellington, C. P. (2002a). The aerodynamics of revolving wings I. Model hawkmoth wings. *J. Exp. Biol.* **205**, 1547-1564.

Usherwood, J. R. and Ellington, C. P. (2002b). The aerodynamics of revolving wings. II. Propeller force coefficients from mayfly to quail. *J. Exp. Biol.* **205**, 1565-1576.

Weis-Fogh, T. (1972). Energetics of hovering flight in hummingbirds and in *Drosophila. J. Exp. Biol.* **56**, 79-104.

Wells, D. J. (1993). Muscle performance in hovering hummingbirds. *J. Exp. Biol.* **178**, 39-57.